Analysis in Sensibility of a Motion Detection Algorithm for Selecting Noise Reduction Methods in X-ray Image Sequences

Lucas Souza e Silva, Filipe Ribeiro Rocha, Lorena Borges Amaral
Cássio Alves Carneiro, Flávia Magalhães Freitas Ferreira, Zélia Myriam Assis Peixoto
Graduate Program in Electrical Engineering
Pontifical Catholic University of Minas Gerais, PUC Minas
Belo Horizonte, Brazil
Email: lucas.souza170@gmail.com

***Abstract*—The quantum noise, intrinsic to the acquisition of X-ray images, becomes more significant during the processes related to fluoroscopy due to its low signal to noise ratio. In this condition, and if there is presence of motion in the image sequence, the use of temporal filtering is restricted, because it will lead to the generation of traces in the resulting filtered images. This artifact can be minimized using purely spatial filtering on regions where motion has been detected. The combination of temporal filtering / spatial filtering results in the hybrid filtering, which is driven by a binary mask of motion detection and it is obtained from the analysis and classification of pixels, based on statistical properties of the image.**

In this sense, this article aims at contributing to the methods of motion detection, presenting new analyzes in the sensibility of a detection algorithm and tests with real images of X-ray examinations. Preliminary results indicate that the filtering process can be improved with the proper choice of parameters of the motion detection mask for different types of medical X-ray procedures, which differ fundamentally by the amount of relative movement among consecutive frames and the contrast among gray intensities in an image sequence, in relation to the static background.

***Keywords*-motion detection; spatial filtering; temporal filtering; hybrid filtering; digital imaging; X-ray;**

I. Introduction

The use of X-ray in medical diagnosis has acquired increasing importance in the identification of diseases, fractures, among others, since its inception. It can be explained by the fact that it is a technology which allows the application of fast, accurate and noninvasive procedures [1].

Considering the risk of anatomical and functional changes in cells, intrinsic in processes involving radiation emissions, lower dosages of X-ray, reduction of exposure time and, at the same time, the improvement of the quality of the resulting images are premises that must be met in those applications that use this technology.

In this perspective, this work intends to contribute with a sensibility analysis of the motion detection mask shown in [2] [3], applied to the noise reduction in X-ray images sequences, obtained in real conditions of such examinations. This algorithm which generates a motion detection mask has been chosen because of its ease implementation in digital hardware based on FPGA (Field Programmable Gate Arrays). These platforms appear to be increasingly common in image and video processing systems which require high rates of data processing [4].

It is important to point out that the temporal filtering techniques produce images with better signal to noise ratio (SNR), compared to results obtained with the application of spatial filtering. However, the first method is not suitable for sequences of moving images because it generates traces as artifacts in the filtered image. In this context, the use of a method of motion detection ensures that the temporal filtering is applied to all pixels of the static portion of a given frame, allowing the spatial filtering to the other pixels.

Firstly, this paper presents a description of the noise present in X-ray images based on related works. Then, it describes the hybrid filtering algorithm shown in [2] [3] with emphasis on the steps of classifying pixels for the composition of the binary mask of movement. Finally, it presents an analysis in the performance of the motion detection process and the impact of the filtering process on real X-ray images.

II. The noise present in X-ray images

The source of X-ray is the major responsible for the noise present in X-ray images. It produces the quantum noise which contributes with random and non-homogeneous distribution of photons in the receiving surface of the Flat Panel Detector (FPD), in current equipment. Because of this deficiency, the signal to noise ratio is not the same for the whole image, then, areas of greater density of photons have a higher SNR than those areas where the density of photons is reduced.

Once the fluoroscopy provides X-ray images with low contrast due to its reduced associated radiation dosage, it is necessary to enhance this contrast through the application of a histogram equalization technique. Nevertheless, this operation also amplifies the noise intensity in the resulting images of the examinations.

From the studies realized in current literature, as in [2] [3] [5] [6] [7] [8], it can be observed that the X-ray image noise is, usually, modeled through the Gaussian distribution. Following the methodology adopted by these

mentioned studies, this work chose to approximate the noise present in X-ray images by a Gaussian distribution, according to the expression:

$$P(k) = \frac{1}{\sqrt{2\pi\sigma^2}} e^{\frac{-(k-\mu)^2}{2\sigma^2}} \quad (1)$$

Where μ and σ^2 are the sample mean and the sample variance, respectively.

It is worth mentioning a recent alternative representation of noise, where its model is empirically constructed from the difference between an image obtained with high dosage of radiation, taken as reference, and the image acquired under normal test, with low X-ray dose and, therefore, lower SNR [9] [10].

III. Motion Detection and Hybrid Filtering Algorithms

Towards an easier digitally or via software implementation, the filtering of digital images is more commonly performed in the spatial and time domains, an alternative to filtering methods in the spatial frequencies domain. If the neighborhood of a pixel, corresponding to the domain used in its filtering, is defined in a single image frame, the filtering process is called spatial and it is more suitable for dynamic regions of an image sequence, where relative motion among consecutive frames is identified. When this neighborhood is defined among adjacent frames of an image sequence, it is said that the filtering process is temporal, which is best used on static regions of this sequence of images. Although the temporal filtering presents a better performance on the elimination of noise, its application in motion areas causes the appearance of tracks in the filtered image, associated with changing in location of the objects.

In this context, it is defined the hybrid filtering, which consists of the selection, pixel by pixel, between the result of spatial filtering or temporal filtering, driven by the presence or absence of movement in each unit of the image. The identification of motion in pixels of an image frame is commonly performed by the statistical characterization of a group of pixels selected according to their gray intensity in the noisy frame.

This operation requires a method for motion detection among adjacent frames of a sequence of X-ray images. The motion detection algorithm, initially proposed by [2] [3], and the implementation of hybrid filtering are shown in flow diagram of Fig. 1 and it is described by the following steps:

1) Generation of an absolute difference image between the current frame and the previous noisy frame already filtered;
2) Definition of the number K of gray levels intervals S_i, $i = 0, 1, ..., K-1$, to be considered for the statistical characterization of the luminous intensity of the image. Table I shows the intensity range varying from 0 to 255, used for 8-bit monochromatic images, divided into eight ranges of gray levels;
3) Allocation of each pixel of the current noisy frame in its corresponding interval S_i,$i = 0, 1, ..., K-1$;

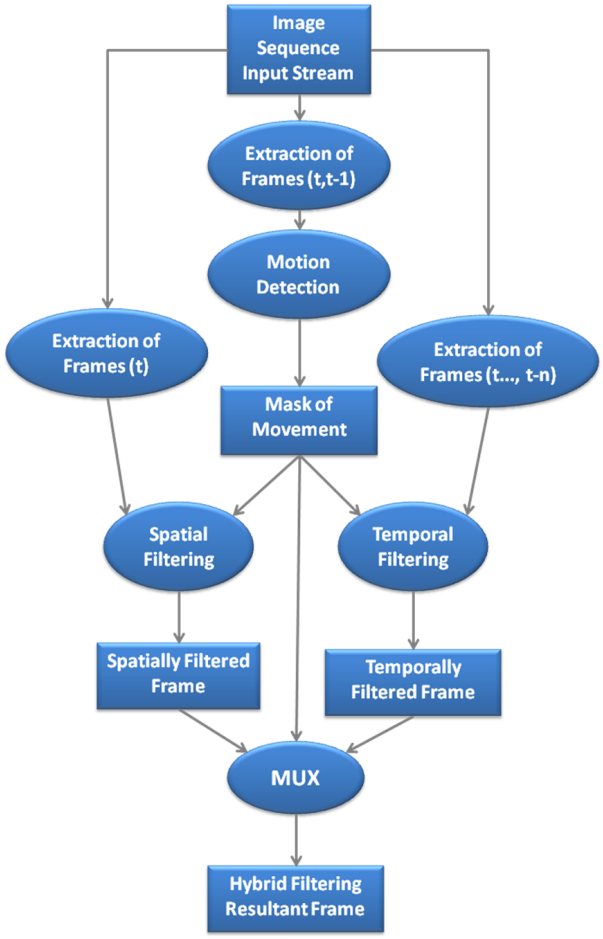

Fig. 1. Flowchart of the hybrid filtering algorithm

4) Calculation of the standard deviation of pixels allocated to each interval S_i,$i = 0, 1, ..., K-1$, aiming at modeling the average variation of gray levels placed in each interval;
5) Application of the decision rule in expression (2) to classify each pixel in the noisy image frame as static (hypothesis H_0) or motion (H_1). The rule consists in comparing each pixel located at position (x, y) in the absolute difference image, with the value of three standard deviations calculated for the range S_i where the pixel with corresponding position is located in the current noisy frame. If the pixel value of the difference image is greater than three standard deviations, H_1 is selected, otherwise, H_0 is chosen

$$\left| i_t(x,y) - i_{(t-1)}(x,y) \right| \underset{H_0}{\overset{H_1}{\gtrless}} 3\sigma_{S_i}, \quad \text{if } i_t(x,y) \in S_i \quad (2)$$

Where $i_t(x, y)$ and $i_{(t-1)}(x, y)$ correspond to the pixel located at position (x, y), respectively, in the image frames sampled at instants (t) e $(t-1)$ and σS_i corresponds to

the standard deviation calculated for the interval S_i.

6) Generation of a binary image called mask of movement (or motion detection mask), in which the pixel located at position (x, y) is assigned with value "0" if the pixel of the difference image in the corresponding position has been classified as static and value "1", if the pixel of the difference image in the corresponding position has been classified as motion pixel in step 5;
7) Application of temporal or spatial filtering in the group of pixels classified as static pixels or pixels of motion, respectively;
8) Formation of the resulting filtered image by selecting and multiplexing the outputs of the temporal and spatial filters, pixel by pixel, considering the original position (x, y) of the filtered pixels.

A. Setting the characteristics of the motion detector

In order to become the motion detection algorithm adapted to the image characteristics, some setting options related to the spectral resolution of the images - number of bits per pixel (γ) - were included as well as the choice of K intervals related to the amount of gray levels to be considered in motion detection. Thus, the index i which assigns the range Si in which each pixel of the current noisy frame is being allocated is equal to $(N-1)$, where N corresponds to the integer part of the division of the pixel intensity I by a factor β, according to equations (3) and (4), which floor(x) returns the greatest integer value less than or equal to x.

$$\beta = \frac{(2^{\gamma})}{K} \tag{3}$$

$$N = floor\left(\frac{I}{\beta}\right) \tag{4}$$

B. Spatial and temporal filtering

As shown in the flowchart depicted in Fig. 1, in the final step, the hybrid filtering algorithm includes the temporal and spatial filters, that are enabled, or not, depending on the result, pixel by pixel, of the binary mask of movement. Equations (5) and (6) indicate, respectively, the spatial filtering of medium in the two-neighboring configuration and a first order recursive temporal filtering [11]. In this case, If_t^{temp} and $If_{(t-1)}^{temp}$ correspond, respectively, to the results of temporal filtering applied to the frames at instants t e $(t-1)$, $If_t^{spatial}$ correspond to the application of the spatial filtering in the frame at instant t and it correspond to the current noisy frame.

$$If_t^{spatial} = \frac{[i_t(x-1,y) + i_t(x,y)]}{2} \tag{5}$$

$$If_t^{temp} = \frac{[If_{(t-1)}^{temp}(x,y) + i_t(x,y)]}{2} \tag{6}$$

TABLE I
PIXELS OF AN 8-BITS MONOCHROMATIC IMAGE DISTRIBUTED IN K= 8 GRAY LEVELS INTERVALS (S_I)

Si	Range of intensities of pixels
S0	0-31
S1	32-63
S2	64-95
S3	96-127
S4	128-159
S5	160-191
S6	192-223
S7	224-255

IV. SIMULATIONS RESULTS

The algorithm described was implemented in MatLab Environment, aiming at analyzing the performance of algorithms for motion detection and filtering applied to monochromatic images acquired in real X-ray examinations.

A. Spatial and Temporal Filtering applied in phantoms

Preliminary tests of temporal and spatial filters were conducted with images from tests that replicate cine-fluoroscopy and radiography examinations applied to phantoms, which are structures that simulate the human body with different densities and thicknesses. We adopted the following procedure:

1) The phantom images acquired with high X-ray dosage were treated as reference images due to their high signal to noise ratio and images which simulate the actual conditions of the examinations (low doses of X-ray) were obtained from the inclusion of Gaussian noise;
2) The peak signal to noise ratio (PSNR) was calculated to quantify the difference between the images corrupted with noise and the reference images. This metric was chosen instead of the signal to noise ratio (SNR), because it is easier calculated and is widely used in the literature;
3) Application of filtering algorithms on the noisy frames;
4) Calculation of PSNR between the filtered frames and reference images;
5) Evaluation of filtering methods applied by analyzing the values calculated in steps 2 and 4 and subjective inspection of the results;
6) Evaluation of how the number of frames and recursion influence on the final results of temporal filtering.

To illustrate the application of this methodology, Fig. 2 presents some stages related to the average spatial filtering techniques applied on a phantom image. In addition, Table II presents some results for temporal filters applied to the phantoms by the PSNR and relative gain in relation to the noisy image.

As expected, it was found that the increase in the number of samples improves the performance of both, recursive and non-recursive filters. Nevertheless, it must be observed if this improvement justifies the increased complexity of implementation in digital hardware platforms, as those based on FPGA.

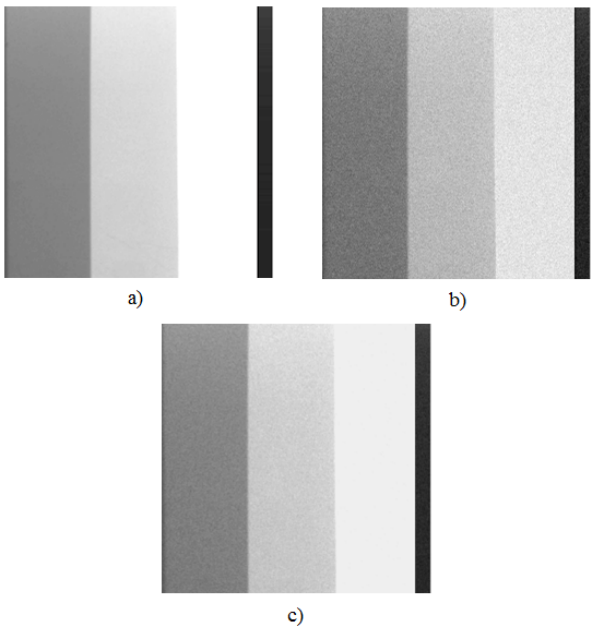

Fig. 2. Spatial Filtering: (a) Reference image acquired by the technique of fluoroscopy. (b) Image corrupted with Gaussian noise. (c) Output of the average filter

TABLE II
RESULTS OF MEDIUM TEMPORAL FILTERING APPLIED ON FLUOROSCOPY IMAGES.

PSNR of the noisy image = 38.3425 dB		
Technique	PSNR (dB)	Relative Gain
Non-recursive filter of 2 samples	39.9762	1.6337
Recursive filter of 2 samples	40.6493	2.3068
Non-recursive filter of 3 samples	40.5987	2.2562
Recursive filter of 3 samples	40.6576	2.3151
Non-recursive filter of 4 samples	40.8130	2.4705
Recursive filter of 4 samples	40.8872	2.5447

B. Hybrid filtering applied on actual X-ray images

Initially, the sequences of actual images obtained from the FPD, whose extension file is ".raw" and resolution of 14 bits, were visually classified for different parts of the human body and the intensity of X-ray, which defines the level of contrast of the image intensities.

Then, these images was subjected to the hybrid filtering procedure described and the algorithms performance was evaluated based on the sensibility of motion detection relative to the number of ranges of gray levels, as well as the number of frames and pixels to be considered in the temporal and spatial filters, respectively.

In Fig. 3, (a) is the sampled image frame at the instant (t-1), already filtered by using the method in question and (b) is the noisy frame sampled at instant (t). After being subjected to the hybrid filtering process, (b) originates the filtered frame (f). Figure Fig. 3 also shows the results corresponding to the partial filtering the noisy frame sampled at instant (t): in (c) purely spatial filtering, using the technique two-neighboring, described in [11], and (d), purely temporal filtering, using a non-recursive of two samples method. It is noticed that the spatial filtering tends to eliminate spatial high frequency components of the image (transitions or edges) and, therefore, the filtered image has a spatial effect of homogenization. In temporal filtering, since there was relative motion between the frames sampled at instants (t) and $(t-1)$, it is possible to observe the appearance of traces, nonexistent in the noisy frame. In medical imaging, this effect can be critical, since these objects can mask the real conditions of the patients and induce the doctor to inaccurate and incorrect diagnosis. The binary mask of movement, resulting from the classification of each noisy pixel as static or moving, is depicted in (e) where white pixels are motion pixels and the black pixels are static pixels. After selection pixel by pixel of the proper output filter, based on the motion mask, it is obtained the final result of the hybrid filtering, shown in (f).

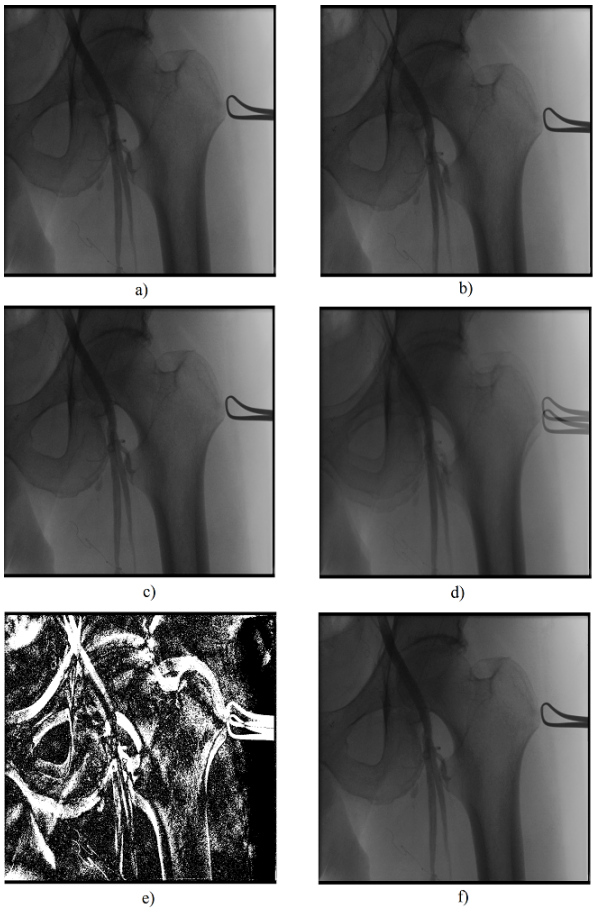

Fig. 3. (a) Previous filtered frame, (b) Current noisy frame, (c) Result of spatial filtering, (d) Result of temporal filtering, (e) Binary mask of movement and (f) Result of hybrid filtering.

C. Evaluation of the sensibility of the motion detection algorithm

The tests were performed with the algorithm with several sequences of actual X-ray, which are listed in the first column

of Table III and they correspond to tests relating to different parts of the human body, such as orthopedic examinations, hemodynamics in heart, brain scans, and lung examinations, among others. The sequences contain different numbers of frames, a higher or lower intensity and also different quantity of relative movement among adjacent frames, as it was observed from a subjective evaluation of the change in location of objects in the image sequence (see second and third columns of Table III, respectively).

For comparison, the image sequences were classified according to the amount of movement and contrast of intensity between the moving objects and the static background. It is important to point out that among the main causes of motion in such examinations are the injection of contrast in the blood vessels (which refers, of course, to the increase of the contrast in intensity between the blood vessels to be observed in examinations of hemodynamics and other body tissues X-rayed), the involuntary movement of internal organs of the body, the movement of the instruments used in examinations and patient movements during procedures.

The evaluation of the sensibility of the motion detection algorithm was carried out in order to correlate the number of gray levels to be used by the algorithm and characteristics of the examinations related to the causes of motion in the images and contrasts of intensity among bodies in motion and the static background.

Following this methodology, the amount of movement in the observed image sequences listed in Table III, from a qualitative inspection, was classified as follows:

- Low: concentrated movement, when a contrast liquid is injected into the main vein;
- Medium: expansive movement, when a contrast liquid is injected into the main vein and small vessels;
- High: generalized movement, when the contrast liquid is injected into the vein and small vessels, as well as other objects are also moving in the image sequence, such as instruments used in the procedure, or even the patient himself.

Likewise, the binary masks of movement were evaluated by a subjective analysis and were classified according to two distinct parameters: (i) the sensibility to detect true movement among consecutive frames in an image sequence, correctly represented by white pixels in the mask and (ii) the misclassification of noise as motion pixels, which is represented by white pixels when they actually should be black pixels.

Regarding the first parameter, the following classifications can be distinguished:

A Motion detection is non-existent;
B Low intensity of detection;
C Medium intensity of detection;
D High intensity of detection.

According to the second parameter, the binary masks of movement were classified as follows:

1) There was no mistaken detection of noise;
2) Little erroneous detection of noise, just in a few frames;
3) Little erroneous detection of noise, but in all frames;
4) Excessive erroneous detection of noise in all frames.

TABLE III
EVALUATION OF THE MOTION DETECTION ALGORITHM.

	Actual Images		Motion Masks with K equals to				
	Qty of frames	**Movement**	**8**	**16**	**32**	**64**	**128**
0	5	Low	A-1	B-1	C-1	**D-1**	D-3
1	8	Low	A-1	B-1	B-1	**D-2**	D-3
2	15	Medium	A-1	B-1	C-1	**D-2**	D-3
3	51	High	B-1	C-2	**D-3**	D-4	D-4
4	26	High	B-1	C-1	**D-3**	D-4	D-4
5	48	High	C-1	**D-2**	D-3	D-4	D-4
6	41	High	B-1	C-2	**D-3**	D-4	D-4
7	170	High	B-1	C-2	**D-4**	D-4	D-4
8	8	Low	A-1	B-1	B-1	B-2	**C-3**
9	6	Low	A-1	B-1	B-1	**D-3**	D-4
10	7	Medium	B-1	B-1	C-1	**D-2**	D-3

The positions outlined in Table III indicate the number of intervals Si that presented the best result for each database image sequence. It is noteworthy that, according to these parameters used for the classification of the masks, those evaluated as D-1 would be the ideal mask, since they show the highest percentage of pixels correctly classified as static or moving. The worst masks are those classified as A-4, when all pixels identified as movement are, in fact, noise.

The relation between the classification of movement in real images (low, medium or high) with the optimal parameter K (number of intervals of gray levels) of the motion detection algorithm, in general, can be related as follows: for sequences with movement classified as low or medium, a large number of intervals (64 or 128) provided the best results. In the other hand, for sequences classified with high intensity of motion, the best results were obtained with amounts of intermediate gray levels (in this case, 32), which turns it feasible to select different amounts of gray levels in the motion detection algorithm, according to the amount of movement or the contrast of the image sequence. This is explained by the fact that the quantity K is directly related to both parameters used for the classification of masks. If a small K is used, there will be few intervals to distribute the gray intensities of the pixels located in a frame. Thus, the standard deviation will be higher in each range. By comparing the value of the difference image in a certain position with the threshold equal to three standard deviations calculated for the corresponding interval, according to steps 4 and 5 of the hybrid filtering algorithm presented, only very high values in the difference image are classified as moving pixels. Therefore, sequences of low contrast image or with a small amount of movement require a higher value of K, so that there are more ranges of gray levels, the standard deviation at each interval, and consequently the threshold comparison with the values of the image difference, is smaller. Thus, small movements, or movements of objects with low contrast may be detected. Equivalently, if an excessive number of intervals (large K) is used, the noise will most likely be mistakenly characterized as movement.

In further analysis, Fig. 4, Fig. 5 and Fig. 6 show the

standard deviation σS_i (y-axis in the graphs) calculated for each interval Si (i = 1,..., K are the x-axis in the graphs), considering, respectively, to Fig. 4, Fig. 5 and Fig. 6, K = 32, 64 and 128 intervals of gray intensities. The calculation was performed for three different image sequences (sequences 1, 3 and 7 listed in Table III). As anyone can see, within the intermediate gray intervals, which is the concentration of most pixels in the images, the standard deviation of all bands is nearly the same, regardless of the sequence of images. Variations of the standard deviation in the first and the last gray intervals shall be basically the differences of the histograms for each sequence (certain sequences are lighter, other darker). Furthermore, as expected, the increase in K causes an inversely proportional reduction in the value of the standard deviation calculated in each range Si. In other words, by doubling K, the standard deviation falls to half.

This analysis shows an inadequacy in the motion detection algorithm proposed by [3]. First, because the algorithm demands a high processing for calculating the standard deviation at each interval, which increases the latency of the hybrid filtering block, since all pixels of a frame must be read before the standard deviation is computed in each interval and then the values of the difference image are compared to the thresholds calculated. Second, because the level of contrast of the images does not interfere in the standard deviation of the gray levels intervals established. This property is desirable for the composition of a binary mask of movement with a lower probability of error.

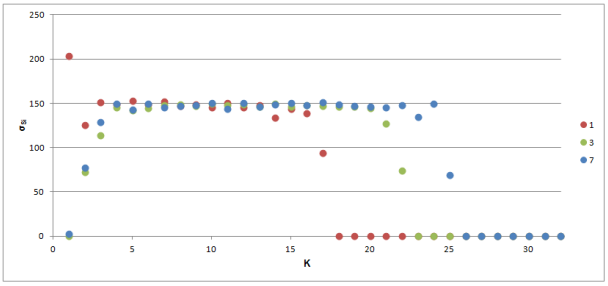

Fig. 4. Standard deviation for each interval of gray levels, assuming a total of 32 intervals to sequences 1, 3 and 7.

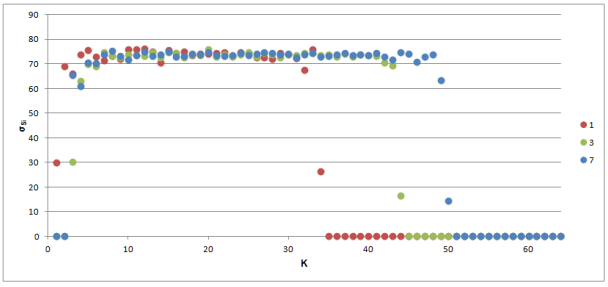

Fig. 5. Standard deviation for each interval of gray levels, assuming a total of 64 intervals to sequences 1, 3 and 7.

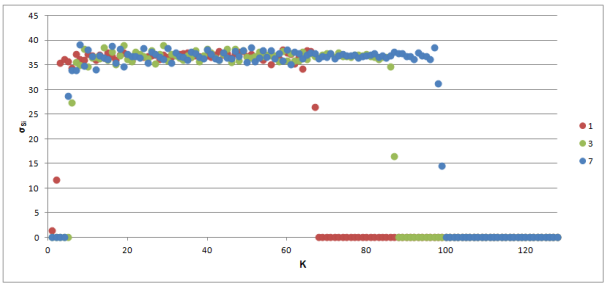

Fig. 6. Standard deviation for each interval of gray levels, assuming a total of 32 intervals to sequences 1, 3 and 7.

V. Final Thoughts

Ultimately, the application of noise reduction techniques in medical imaging allows the doctor to provide safer and faster diagnosis. Furthermore, by reducing the noise intensity in these images, it is possible to reduce patients exposure during examination as well as the doses of radiation the patient is subjected to.

It was found that the application of a hybrid filtering is suitable for this purpose since it selects, pixel by pixel, the proper filtering method to be applied to the noisy image frame, ensuring that the temporal filtering is applied on the static pixels and maximizing the final result in the process of noise reduction.

Considering that motion detection is done separately for each pixel, it does not aim at first to find well-defined regions of motion. However, the probability that a pixel misclassification as static or motion may be minimized by using morphological filters, as erosion and dilation respectively, on the mask of movement [11].

To conclude, as the main contribution of this work, it is emphasized the subjective analysis of the relation between the amount of gray intervals considered by the algorithm of motion detection and the probability of success related to the decision rule, which aims at classifying the pixels as static or movement. In addition, our studies indicate a deficiency of the proposed method for motion detection, by not considering most effectively the characteristics of contrast of the images to the composition of the decision rule. Finally, it is important to keep in mind that the use of real X-ray images contributed to a more detailed analysis of the sensibility of the motion detection algorithm, making it possible to identify fields still open to research in such algorithms.

Acknowledgment

The authors would like to thank the PPGEE (Graduate Program in Electrical Engineering) from PUC Minas (Pontifical Catholic University of Minas Gerais) as well as the Company XPRO Sistemas LTDA, for supplying the real X-ray image sequences and the scolarship for the undergraduate student.

REFERENCES

[1] YU, L., LIU, X., KOFLER, J. M., GIRALDO, J. C. R., QU, M., CHRISTNER, J., FLETCHER, J. G., and MCCOLLOUGH, C. H., "**Radiation dose reduction in computed tomography: techniques and future perspective**," 2009.

[2] HENSEL, M., PRALOW, T., and GRIGAT, R.-R., "**LAST Filter for Artifact-Free Noise Reduction of Fluoroscopic Sequences in Real-Time**," 2008.

[3] HENSEL, M., LUNDT, B., PRALOW, T., and GRIGAT, R.-R., "**Robust and Fast Estimation of Signal-Dependent Noise in Medical X-Ray Image Sequences**," 2006.

[4] SILVA, L. S., OLIVEIRA, I. T., and FREITAS, F. M., "**Implementao de Mdulos de Processamento Digital de Vdeo em Tempo Real Utilizando-se Plataforma Baseada em FPGA. Belo Horizonte**," 2010.

[5] ZHU, H., SUN, W., WU, M., GUAN, G., and GUAN, Y., "**Pre-Processing of X-Ray Medical Image Based on Improved Temporal Recursive Self-Adaptive Filter**," 2008.

[6] CHAN, C. L., KATSAGGELOS, A. K., and SAHAKIAN, A. V., "**Image Sequence Filtering in Quantum-Limited Noise with Applications to Low-Dose Fluoroscopy**," 1993.

[7] FOI, A., TRIMECHE, M., KATKOVNIK, V., and EGIAZARIAN, K., "**Practical Poissonian-Gaussian Noise Moeling and Fitting for Single-Image Raw-Data**," 2008.

[8] WILSON, D. L., JABRI, K. N., and AUFRICHTIG, R., "**Perception of Temporally Filtered X-Ray Fluoroscopy Images**," 1999.

[9] GIRALDO, J. C. R., FLETCHER, J. J., and MCCOLLOUGH, C. H., "**Reduccin del ruido en imgenes de tomografa computarizada usando un filtro bilateral anisotrpico**," 2010.

[10] TABUCHI, M. and YAMANE, N., "**Denoising X-Ray CT Images based on Product Gaussian Mixture Distribution Models for Original and Noise Images**," 1993.

[11] GONZALEZ, R. C. and WOODS, R. E., "**Processamento de Imagens Digitais**," 2010.